PLASTIC DEFORMATION OF SPHERICAL STEEL SHELLS UNDER INTERNAL BLAST LOADING

L. N. Aleksandrov, A. G. Ivanov,
V. N. Mineev, V. I. Tsypkin,
and A. T. Shitov

UDC 620.178.7

Research performed so far on shells subjected to internal blast loading has developed the basic laws of their behavior. The elastic and elastic-plastic response of thin-walled shells filled with water was determined in [1, 2], and of shells filled with air under normal conditions in [3-7].

In the present article we present computational and experimental results of research directed toward finding the laws of behavior of spherical shells of various thicknesses in the region of plastic deformation (up to rupture) under a single internal blast loading.

We have studied the behavior of spherical shells of mass M having inside and outside radii R_{1o} and R_{2o} respectively and wall thickness h_o (Fig. 1), filled with a normal air atmosphere, for an internal explosion of a charge 1 of explosive (EX). The shells 2 were made of steel 35, and annealed to relieve residual stresses in the area of welded joints. The mechanical properties of the shell material were checked by tests of control samples (σ_u = 0.55 GPa, $\sigma_{s(0.2)}$ = 0.30 GPa, δ = 20%).†

Shells having the same inside radius R_{1o} = 153 mm and various wall thicknesses were used in the experiments; some shells were geometrically similar, but scaled down by a factor of 4.

The explosive charges were TH 50/50 (50 wt.% TNT and 50 wt.% hexogen with a density of $1.65 \cdot 10^{-3}$ kg/cm^3) spheres of radius R_3 and mass m, located at the center of the shells, and triggered from the center. Each shell was subjected to only one blast loading.

Following the method described in [8], we used strain gages 3 (Fig. 1) to record the deformation of the shells as a function of time $\varepsilon(t)$. A typical oscillogram of $\varepsilon(t)$ is shown in Fig. 2 (experiment 7). By processing the experimental results for $\varepsilon(t)$ the following quantities were determined: v*, the maximum rate of displacement of the shell walls by differentiating $\varepsilon(t)$; ε^*, the maximum strain of the material at the instant the shell walls stopped or were ruptured ($\varepsilon^* = \Delta R_2^*/R_{2o}$, where $\Delta R_2^* = R_2^* - R_{2o}$; R_{2o} is the initial value of the outside radius of the shell, and R_2^* is the maximum radius in the deformation process); t^* is the time interval between the beginning of loading and the instant the deformation is maximum.

The estimated errors of the determination of the quantities listed are: $v^* \sim \pm 10\%$, ε^* and $t^* \sim$ %5% (for shells which were not ruptured). The dimensions of the shells and the experimental results are listed in Table 1.

In a number of experiments with shells having a relative wall thickness h_o/R_{2o} = 1.67% and 8.1%, the maximum inward velocity of the walls for $t > t^*$ was determined also, and this made it possible, as in [6], to estimate the dynamic yield stress σ_s; it turned out to be $\sim$0.5 GPa.

By processing data from our experiments and [2] we found that the dynamic hardening modulus of St. 35 is relatively small. Therefore, for the relatively small plastic strains ($\varepsilon^* < 5\%$) taking place in the experiments, neglecting the elastic part, the shell material is rigid-plastic with σ_ε = 0.5 GPa.

†σ_u, σ_s, and ε_o are respectively the ultimate strength, the yield stress, and the tensile strain.

Moscow. Translated from Zhurnal Prikladnoi Mekhaniki i Tekhnicheskoi Fiziki, No. 6, pp. 103-108, November-December, 1982. Original article submitted June 26, 1981.

0021-8944/82/2306-0831$07.50

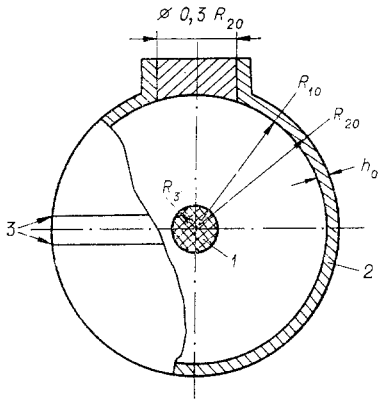

Fig. 1

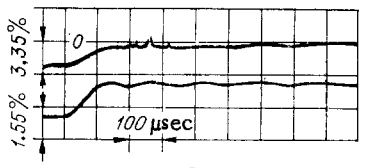

Fig. 2

TABLE 1.

No.	R_{20}, mm	δ,%	m, g	ξ, 10^{-3}	i, 10^5 nsec/m²	η	ε*,% exp.	ε*,% calc.	v*, m/sec exp.	v*, m/sec calc.	t*, μsec exp.	t*, μsec calc.
1			61	10	0,011	0,17	0,5	0,17	20	8,9	80	65
2	155,6	1,67	79	13	0,014	0,32	0,7	0,58	22	22	90	83
3			105	17,4	0,019	0,47	1,8 (p)†	1,5	29	42	150	112
4			460	13,6	0,082	0,24	0,7	0,32	21	19	100	97
5	166,5	8,1	576	17	0,103	0,38	1,2	0,94	25	37	140	123
6			700	20,7	0,124	0,46	1,9	1,9	34	54	160	147
7			945	28	0,168	0,59	3,2 (p)†	4,5	60	94	120	199
8			10,5	19,8	0,030	0,46	1,6	1,6	—	47	—	35
9	41,5	8,1	14,85	28,1	0,043	0,61	5 (p)†	4,6	65	90	50	51

†(p)* — the shell was ruptured in the loading process.

It is assumed also that for relatively small distances from the inner surface of a shell to the charge $2.5 < R_{10}/R_3 < 7$, the force of the explosion is determined by the character of the reflection of the detonation products (DP) from the shell wall. It is assumed that the relative effect of the leading shock wave in air is small in comparison with the effect of the DP.

Clearly this assumption will be fairly accurate in the near zone of the explosion when the mass of air involved in the motion is appreciably smaller than the mass of DP.

Taking account of what has been said, in estimating the effect of DP on a shell, we replaced the actual complex-shaped pressure pulse (Fig. 3, $R_{10}/R_3 = 3$, 3.8 and 6.8 for curves 1-3 respectively) by an effective pulse having a constant amplitude equal to the maximum pressure of reflection of DP from the shell, i.e., $p_1 \tau = i$, where τ is the duration of the effective pulse, p_1 is its amplitude, and i is the magnitude of the specific loading impulse.

The values of p_1 for the reflection of DP were determined from the pressure pulse shape at the inner surface of the shell, calculated by computer using the method of [9]. The equation of state used in the calculation was taken from [10] for TH 50/50, and from [11] for air. The maximum pressure of reflection as a function of the relative distance R_{10}/R_3 is shown in Fig. 4. Just as in [12], this relation is satisfactorily approximated by the expression

$$p_1 = A(R_{10}/R_3)^b, \tag{1}$$

where A = 3.2 GPa and b = −2.53 in the range $2.5 < R_{10}/R_3 < 7$.

The accuracy of the approximation can be seen from Fig. 4, where the solid curve is a plot of Eq. (1), and the individual points are the results of the numerical calculation of p_1.

The magnitude of the specific loading impulse was determined from the relation

$$i = ni_0, \text{where } i_0 = \frac{32}{27}\frac{mq^{0.5}}{4\pi R_{10}^2} — \tag{2}$$

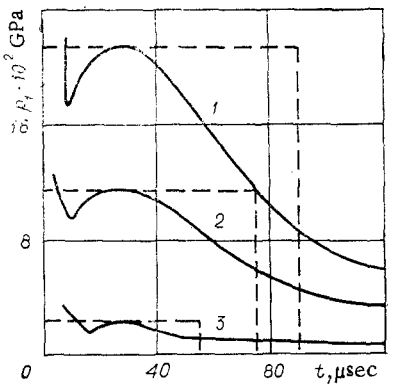

Fig. 3

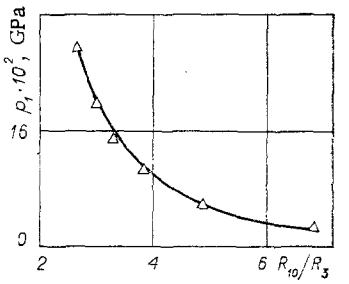

Fig. 4

is the momentum flux of DP through a unit area at a distance R_{10} from the center of the spherical explosive charge of mass m for a caloricity q of the explosive, and n is a factor taking account of the efficiency of the reflection of DP from the wall [13].

By considering the reflection of a layer of material with an acoustic impedance $(\rho c)_{DP}$ and a velocity u_{DP} from a layer of material with an impedance ρc, it can be shown that in the acoustic approximation

$$n = 2/((\rho c)_{DP}/\rho c + 1).$$

For $\rho c \gg (\rho c)_{DP}$, which is true for an appreciable expansion of the DP, $n \approx 2$.

Thus, Eqs. (1) and (2) for $n = 2$ give an analytic description of the effective pressure pulse in the near zone of the explosion for $2.5 \leqslant R_{10}/R_3 \leqslant 7$, and determine τ.

The dynamics of a spherical thin-walled shell having a radius R(t), a wall thickness h(t), a material density ρ, and a loading pressure $p_1(t)$ is described by the equation [3] $\rho h\ddot{R} = p_1(t) - 2\sigma_s h/R$.

We simplify this equation for a region in which there are small changes in R.

Expressing R and h in terms of the strain $\varepsilon = \Delta R_2/R_{20}$, the initial radius R_{20}, and the thickness h_0, and neglecting small quantities of higher order, we obtain

$$(1 - 2\varepsilon)\rho h_0\ddot{R} = p_1(t) - (2\sigma_s h_0/R_0)(1 - 3\varepsilon), \text{where } R_0 = (R_{10} + R_{20})/2.$$

Neglecting 2ε and 3ε in comparison with unity for $\varepsilon < 5\%$, we obtain a linear equation describing the motion of a flat plate with a relative mass $m_0 = \rho h_0$ loaded by the pressure $p = p_1(t) - p_2$, where $p_2 = 2\sigma_s h_0/R_0$ is the pressure resisting the motion of the plate.

Taking account of the parameters of the effective loading impulse, we obtain finally

$$m_0\ddot{R} = p, \tag{3}$$

where

$$p = \begin{cases} p_1 - p_2 & 0 \leqslant t \leqslant \tau, \\ -p_2 & t > \tau \ (p_2 = 0 \text{ for } \dot{R} = 0); \end{cases}$$

at $t = 0$ $\dot{R} = 0$, $R = R_0$.

The extremal characteristics of the deformation process can be obtained after integrating Eq. (3):

$$R^* = \frac{i^2}{2m_0 p_2}\left(1 - \frac{p_2}{p_1}\right) + R_0,$$

$$v^* = \frac{i}{m_0}\left(1 - \frac{p_2}{p_1}\right), \quad t^* = \frac{p_1}{p_2}\tau = \frac{i}{p_2},$$

or, introducing $\eta = 1 - p_2/p_1$, we obtain

$$\varepsilon^* = (i^2/(2m_0 p_2 R_{20}))\eta; \tag{4}$$

$$v^* = (i/m_0)\eta; \tag{5}$$

$$t^* = [1/(1 - \eta)]\tau. \tag{6}$$

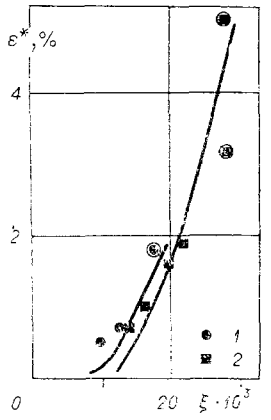

Fig. 5

If $p_1 \to p_2$, and other conditions remain the same, $\eta \to 1$, and Eqs. (4)-(6) take the form

$$\varepsilon^* = i^2/(2m_0p_2R_{20}),\ v^* = i/m_0,\ t^* = i/p_2.$$

In this case a regime of pure impulsive loading exists, and the time characteristics of the impulse are unimportant.

If $p_1 \to p_2$, $\eta \to 0$, and at the same time (for i = const) $\varepsilon^* \to 0$, $v^* \to 0$, and $t^* \to \tau$.

In this case the extremal characteristics of the deformation depend strongly on the relative pressure of the pulse p_1/p_2 or on its relative duration τ/t^*.

Using Eqs. (1), (2), and (4) and obvious relations connecting the mass of the shell and of the charge with their geometry, and making a number of simple transformations, we obtain the expression

$$\varepsilon^* = \frac{\left(\frac{64}{27}\right)^2 q\rho}{2A}\left(\frac{3\rho}{\rho_{EX}}\right)^{\frac{b}{3}}\delta^{1+\frac{b}{3}}(1-\delta)^{-(2+b)}\left(1-\delta+\frac{1}{3}\delta^2\right)^{1+\frac{b}{3}}\xi^{2+\frac{b}{3}}\times$$
$$\times\left[\frac{A}{2\sigma_s}\left(\frac{3\rho}{\rho_{EX}}\right)^{-\frac{b}{3}}\delta^{-\left(1+\frac{b}{3}\right)}(1-\delta)^b\left(1-\frac{\delta}{2}\right)\left(1-\delta+\frac{\delta^2}{3}\right)^{-\frac{b}{3}}\xi^{-\frac{b}{3}}-1\right].$$

For thin shells ($\delta \ll 1$) this simplifies to

$$\varepsilon^* = \left(\frac{32}{27}\right)^2\frac{q\rho}{\sigma_s}\xi^2\left[1-\frac{2\sigma_s}{A}\left(\frac{3\rho}{\rho_{EX}}\right)^{\frac{b}{3}}\delta^{1+\frac{b}{3}}\xi^{\frac{b}{3}}\right], \tag{7}$$

which describes the maximum deformation of the shell as a function of the dimensionless parameters $\xi = m/M$, $\delta = h_0/R_{20}$ which characterize the relative mass and the relative thickness of the shell, and $q\rho/A_1$, ρ/ρ_{EX}, and A/σ_S characterizing the physical parameters of the materials used.

In particular, for St. 35 for $\rho = 7.8\cdot10^{-3}$ kg/cm³, $\sigma_S = 0.5$ GPa, $\rho_{EX} = 1.65\cdot10^{-3}$ kg/cm³, $q = 4.77\cdot10^3$ kJ/kg (TH 50/50), A = 3.2 GPa, and b = −2.53, Eq. (7) takes the form

$$\varepsilon^* = 1.05\cdot10^2\xi^2[1 - 3.3\cdot10^{-2}\delta^{0,157}\xi^{-0.843}]. \tag{8}$$

The values of ε^*, v^*, and t^* calculated with Eqs. (8), (5) and (6) are compared with the experimental results in Table 1, where the values of η listed correspond to the loading conditions.

Figure 5 shows the calculated dependence of ε^* on ξ for various values of the relative thickness δ [1) 1.67%; 2) 8.1%]. For comparison the figure also shows the experimental values of ε^*. Points enclosed in circles correspond to rupture of the shell. A comparison of the calculated and experimental values shows satisfactory agreement (10-20%) for $\xi \geqslant 13\cdot10^{-3}$.

For deformations which are nearly elastic, the accuracy of the description falls outside the 20% limit. This is evidently due to the fact that the computational scheme used a rigid-plastic model of the material with a value of the yield stress independent of the strain rate, and also neglected the initial elastic part. The possibility of a change of the yield stress with a change in strain rate has been shown experimentally in [14]. The high-intensity part

of the pulse corresponding to a shock wave in air was also neglected. All that has been said leads to calculated values of ε^* which are smaller than the experimental for small values of ξ.

The results of experiment 7 lie somewhat outside the estimated error limits. The difference between calculation and the results of experiment 7 is accounted for by the premature rupture of the shell before it reached maximum deformation corresponding to the loading regime given in Table 1. This can be seen from a comparison with experiment 9 which had the same input parameters as experiment 7 ($\xi \approx 28 \cdot 10^{-3}$, $\delta = 8.1\%$).

The computational scheme used also satisfactorily describes the kinematic characteristics of the process v^* and t^* (Table 1).

We note that calculation and experiment yield a value of the relative mass $\xi \approx 9 \cdot 10^{-3}$ which is weakly dependent on the relative thickness δ at which there is a sharp bend in the $\varepsilon^*(\varepsilon)$ curve. The region $\xi < 9 \cdot 10^{-3}$, which is of particular practical interest, corresponds to small plastic deformations which are nearly elastic. For $\xi > 9 \cdot 10^{-3}$ there is a rapid increase in deformation with increased loading clear up to rupture at $\varepsilon^* \sim 2$-3%, depending on the relative thickness of the shell.

Thus, our experimental results show that a simple physical model gives a satisfactory analytic description of the parameters of plastic deformation of spherical shells of mild steel under internal symmetric loading by the explosion of a charge of TH 50/50.

LITERATURE CITED

1. J. F. Proctor, "Containment of explosions in water-filled right-circular cylinders," Exp. Mech., 10, 458 (1970).
2. V. I. Tsypkin, A. G. Ivanov, et al., "Effects of scale, geometry, and filler on the strength of steel vessels of pulsed loads," At. Energ., 41, 303 (1976).
3. W. E. Baker and F. J. Allen, "The response of elastic spherical shells to spherically symmetric internal blast loading," in: Proc. Third U.S. Nat. Congr. on Appl. Mech., Providence (1958).
4. A. F. Demchuk, "A method for designing explosion chambers," Prikl. Mekh. Tekh. Fiz., 9, 47 (1968).
5. W. E. Baker, "The elastic-plastic response of thin spherical shells to internal blast loading," J. Appl. Mech., 27, No. 1 (1960).
6. A. G. Ivanov, S. A. Novikov, and V. A. Sinitsyn, "The behavior of steel shells when charges of explosives detonate inside them," Prikl. Mekh. Tekh. Fiz., 9, 94 (1968).
7. S. I. Bodrenko, B. L. Glushak, S. A. Novikov, V. A. Sinitsyn, and A. M. Cheverkin, "Computational-experimental study of the behavior of a closed spherical shell when a spherical charge of explosive material is exploded inside it," in: Abstracts of Papers of Second All-Union Symp. on Impulsive Pressures [in Russian], Moscow (1976).
8. A. T. Shitov, V. N. Mineev et al., "A wire transducer for the continuous recording of large deformations in the dynamic loading of structures," Fiz. Goreniya Vzryna, No. 2 (1976).
9. V. A. Batalov, V. A. Svidinskii, V. I. Selin, and V. N. Sofronov, Program 7 for Solving One-Dimensional Gasdynamic and Elastic-Plastic Problems in the Mechanics of a Continuous Medium, In: Problems of Atomic Science and Engineering, Ser. Methods and Programs for the Numerical Solution of Problems of Mathematical Physics No. 1 (1) [in Russian], TsNIIatominform, Moscow (1978).
10. M. V. Zhernokletov, V. N. Zubarev, and G. S. Telegin, "Expansion isentropes of the explosion products of condensed explosives," Prikl. Mekh. Tekh. Fiz., 10, 127 (1969).
11. N. M. Kuznetsov, Thermodynamic Functions and Shock Adiabats of Air at High Temperatures [in Russian], Mashinostroenie, Moscow (1965).
12. J. Ahrens and R. Kovach, "Explosive gas blast: the expansion of detonation products in vacuum," J. Appl. Phys., 42, 815 (1971).
13. K. P. Stanyukovich (editor), Physics of an Explosion [in Russian], Nauka, Moscow (1975).
14. M. J. Forrestal and M. Sagartz, "Elastic-plastic response of 304 stainless steel beams to impulse loads," J. Appl. Mech., 45, 685 (1978).